Microbiota-induced tertiary lymphoid tissues aggravate inflammatory disease in the absence of RORγt and LTi cells

Matthias Lochner, Caspar Ohnmacht, Laura Presley, Pierre Bruhns, Mustapha Si-Tahar, Shinichiro Sawa, Gérard Eberl

Microbiota-induced tertiary lymphoid tissues aggravate inflammatory disease in the absence of RORγt and LTi cells

Matthias Lochner,[1,4,5] Caspar Ohnmacht,[1,4] Laura Presley,[1,4] Pierre Bruhns,[2,6] Mustapha Si-Tahar,[3,7] Shinichiro Sawa,[1,4] and Gérard Eberl[1,4]

[1]Lymphoid Tissue Development Unit, [2]Unité d'Allergologie Moléculaire et Cellulaire, and [3]Unité de Défense Innée et Inflammation, Institut Pasteur, 75724 Paris, France
[4]URA1961, Centre National de la Recherche Scientifique, 75724 Paris, France
[5]Institute of Infection Immunology, Twincore, Centre for Experimental and Clinical Infection Research, Medical University Hannover and Helmholtz Centre for Infection Research, 30625 Hannover, Germany
[6]INSERM U760, and [7]INSERM U874, 75724 Paris, France

The programmed development of lymph nodes and Peyer's patches during ontogeny requires lymphoid tissue inducer (LTi) cells that express the nuclear hormone receptor RORγt. After birth, LTi cells in the intestine cluster into cryptopatches, the precursors of isolated lymphoid follicles (ILFs), which are induced to form by symbiotic bacteria and maintain intestinal homeostasis. We show that in RORγt-deficient mice, which lack LTi cells, programmed lymphoid tissues, ILFs, and Th17 cells, bacterial containment requires the generation of large numbers of tertiary lymphoid tissues (tLTs) through the activity of B cells. However, upon epithelial damage, these mice develop severe intestinal inflammation characterized by extensive recruitment of neutrophils and IgG+ B cells, high expression of activation–induced deaminase in tLTs, and wasting disease. The pathology was prevented by antibiotic treatment or inhibition of lymphoid tissue formation and was significantly decreased by treatment with intravenous immunoglobulin G (IVIG). Our data show that intestinal immunodeficiency, such as an absence in RORγt-mediated proinflammatory immunity, can be compensated by increased lymphoid tissue genesis. However, this comes at a high cost for the host and can lead to a deregulated B cell response and aggravated inflammatory pathology.

CORRESPONDENCE
Gérard Eberl:
gerard.eberl@pasteur.fr

Abbreviations used: DSS, dextran sulfate sodium; iBALT, inducible bronchus-associated lymphoid tissue; ILF, isolated lymphoid follicle; IVIG, i.v. IgG; LT, lymphotoxin; LTi, lymphoid tissue inducer; NOD, nonobese diabetic; PP, Peyer's patch; tLT, tertiary lymphoid tissue.

In mammals, the development of LNs and Peyer's patches (PPs) is programmed during ontogeny in the sterile environment of the fetus (Mebius, 2003). In contrast, isolated lymphoid follicles (ILFs) are induced to develop after birth in the intestinal lamina propria by the colonizing bacterial microbiota (Hamada et al., 2002; Pabst et al., 2006; Bouskra et al., 2008). The development of both types of lymphoid tissues is initiated by lymphoid tissue inducer (LTi) cells, which express and require the nuclear hormone receptor RORγt for their generation (Eberl and Littman, 2004; Eberl et al., 2004). In the fetus, LTi cells aggregate in LN and PP anlagen where they activate stromal cells through membrane-bound lymphotoxin (LT) $\alpha_1\beta_2$ and LTβR interaction, which results in the expression of adhesion molecules and chemokines involved in the recruitment and organization of lymphocytes (Mebius, 2003).

After birth, LTi cells cluster into cryptopatches (CPs) located between intestinal crypts. Bacteria activate CPs through the shedding of peptidoglycans recognized by NOD-1 in epithelial cells and the release of β-defensin-3 and CCL20 which activate CCR6+ LTi cells and B cells (Bouskra et al., 2008). As a result, CPs collect B cells through an LTβR-dependent mechanism and form ILFs (Lorenz et al., 2003).

Tertiary lymphoid tissues (tLTs), which resemble ILFs (Eberl and Lochner, 2009), develop in a variety of inflammatory lesions both in mouse and man (Aloisi and Pujol-Borrell, 2006). Upon infection with influenza A virus, mouse lungs develop large numbers of inducible
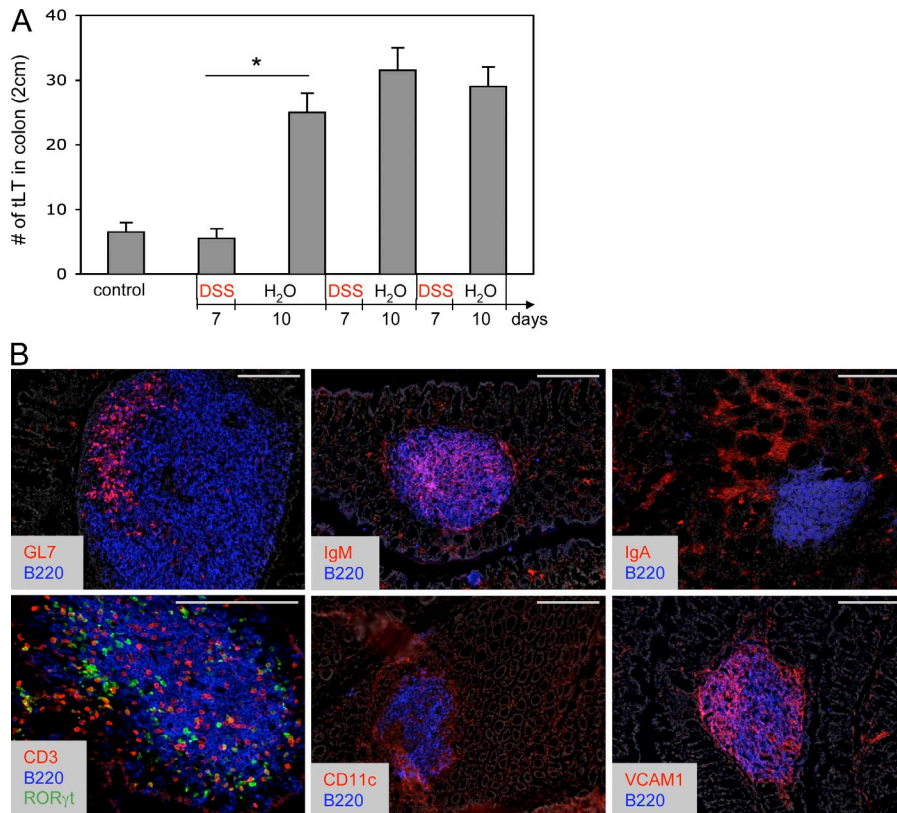
Figure 1. Supernumerary and mature tLTs induced by DSS–mediated colitis. (A) Quantification of tLTs in the colon of wild-type mice before and after multiple cycles of DSS treatment. During each cycle, mice were treated with DSS for a period of 7 d, followed by a 10-d recovery period without DSS. Data are shown for one representative experiment out of two with three mice per group. Statistical significance was assessed by the paired Student's t test. *, P < 0.05. Error bars are SD. (B) Structure of colonic tLTs in sections of colons from wild-type mice after two cycles of DSS treatment. Sections were stained with the indicated antibodies and with DAPI for nuclear staining (shown in gray). RORγt is visualized through GFP expression in $Rorc(gt)$-Gfp^{TG} reporter mice. Bars, 200 μm.

bronchus–associated lymphoid tissues (iBALTs) that promote local immunity and memory to the virus (Moyron-Quiroz et al., 2004, 2006). The formation of iBALT is independent of RORγt+ LTi cells. In that context, LTi function may be performed by abundant effector lymphocytes, such as B cells, that are recruited to the infected lung and, similar to LTi cells, express $LT\alpha_1\beta_2$ (Ansel et al., 2000). In the pancreas of aged nonobese diabetic (NOD) mice, tLTs develop that provide a positive-feedback loop to local inflammation and exacerbate the pathology (Lee et al., 2006). The requirement for LTi cells in the formation of pancreatic tLTs has not been formally assessed, but central to this process is the recruitment of islet antigen–specific T cells. In that case, the ligand activating LTβR on stromal cells is not $LT\alpha_1\beta_2$ but LIGHT (TNFSF14). During intestinal inflammation induced by dextran sulfate sodium (DSS), a high number of tLTs are induced in mice that lack LNs and PPs and the disease is aggravated (Spahn et al., 2002). It was suggested that the pathological inflammation resulted from a failure to engage regulatory pathways in the absence of LNs. The role of LTi cells has not been investigated in that model.

Recent studies show that the IL-17–IL-23 signaling pathway is involved in several chronic inflammatory pathologies, including colitis. IL-23, a cytokine produced by DCs, monocytes and macrophages (Kastelein et al., 2007) and shown to be essential in several experimental colitis models in mice (Uhlig and Powrie, 2009), promotes maturation of proinflammatory Th17 cells and blocks the production of regulatory

IL-10 (McGeachy et al., 2009). Most persuasively, a gain-of-function mutation in the IL-23R predisposes patients to the development of inflammatory bowel disease (Duerr et al., 2006). Th17 cells, which depend on RORγt for their generation (Ivanov et al., 2006), have been shown to be required for disease development in an adoptive transfer model of colitis (Leppkes et al., 2009). Furthermore, IL17R–deficient mice are resistant to trinitrobenzenesulfonic-induced colitis, even in the presence of increased levels of IL-12 and IFN-γ (Zhang et al., 2006). It is therefore suggested that antagonists of IL-17R and RORγt could prevent colitis. However, other models of colitis are associated with a Th1 type or a Th2 type of immune responses, which may limit the effectiveness of a therapeutic targeting of the IL-17/23 pathway (Uhlig and Powrie, 2009).

In this paper, we demonstrate that tLTs can be induced both in influenza A–infected lungs and during colitis in the absence of RORγt and LTi cells. Instead, in the DSS model of mouse colitis, we show that the formation of tLTs is dependent on LTβ expressed by B cells. The lack of Th17 cells, as well as the lack of other populations of IL-17– and IL-22–producing Tγδ cells and innate lymphoid cells in RORγt-deficient mice (Ivanov et al., 2006; Satoh-Takayama et al., 2008; Sanos et al., 2009), does not protect mice from inflammatory disease. On the contrary, the absence of RORγt+ cells to contain the intestinal microbiota is compensated by the formation of a large number of tLTs that leads to severe inflammatory pathology upon epithelial damage, which is characterized by increased B cell recruitment and differentiation. Disease progression is prevented by concomitant treatment of the mice with a broad spectrum antibiotic cocktail and with an antagonist to the LTβR that blocks the formation of tLTs and is mitigated by treatment with i.v. IgG (IVIG), which inhibits B cell–induced
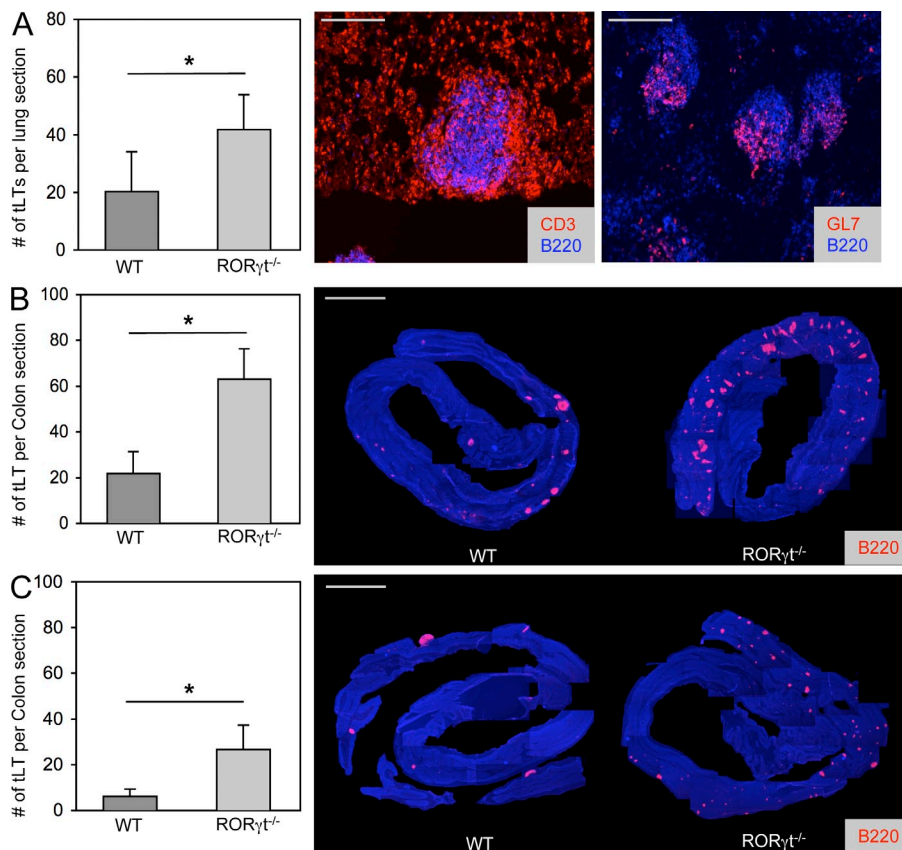
Figure 2. tLTs form in the absence of LTi cells. (A) Quantification of influenza virus A–induced iBALT. RORγt$^{-/-}$ or wild-type control mice were infected intranasally with 50 pfu influenza virus A and sacrificed 3 wk later. Histograms show mean numbers of lymphoid follicles in sections of whole lungs. Data shown are the mean for seven mice per group from two independent experiments. *, P < 0.05. Sections were stained with the indicated antibodies. Bars, 200 µm. (B and C) Quantification of tLTs in the colon of RORγt$^{-/-}$ and wild-type control mice. The number of colonic tLTs was assessed as described in Materials and methods and is indicated as the mean number of tLTs per whole colon section. Data shown for adult mice that were either treated with two cycles of 2.5% DSS (B) or left untreated (C). Figures show data compiled from 10–15 mice per group from three independent experiments. *, P < 0.001. Histology shows representative colon samples from RORγt$^{-/-}$ or wild-type control mice either treated with two cycles of 2.5% DSS or left untreated. Sections were stained with anti-CD45R/B220 antibodies to visualize tLTs and DAPI for nuclear staining. Single pictures of 100× magnified sections were assembled to generate an integral view of a colon. Bars, 0.5 cm. Statistical significance was assessed by the paired Student's t test. Error bars are SD.

inflammatory responses (Nimmerjahn and Ravetch, 2008). Our data indicate that inhibition of the Th17 pathway and of the normal function of lymphoid tissues may exacerbate inflammatory bowel disease through the generation of tLTs and a deregulated B cell response.

RESULTS

The formation of mature tLTs during intestinal inflammation

It was previously reported that colitis induced by 7 d of DSS oral treatment did not induce significant numbers of tLTs when compared with mice receiving water (Spahn et al., 2002). We confirm this observation but observed a marked increase in the number of tLTs after a 10-d period of rest that followed the initial 7 d of DSS (Fig. 1 A). The number of tLTs increased only marginally upon a second cycle of DSS treatment, followed by another rest period, and remained stable during subsequent cycles of treatment. These tLTs were significantly larger than ILFs found in untreated mice. Yet, like conventional ILFs (Hamada et al., 2002; Eberl and Littman, 2004), these structures were composed of a well defined B cell follicle surrounded by a shell of DCs and contained mostly IgM$^+$ B cells, a germinal center, dispersed LTi cells, and T cells, but no defined T cell zone (Fig. 1 B). Stromal cells expressed VCAM-1, which is typical of stromal cells found in lymphoid tissues, collectively termed lymphoid stromal cells (Honda et al., 2001; Peduto et al., 2009).

The LTi–independent formation of tLTs

Even though the generation of LTi cells and the subsequent development of LNs, PPs, and ILFs require expression of RORγt (Eberl and Littman, 2004; Eberl et al., 2004), tLTs induced by influenza A virus infection of the lungs, termed iBALT, develop normally in RORγt-deficient mice (Moyron-Quiroz et al., 2004). In NOD mice, the formation of tLTs in the inflamed pancreatic islets depends on LIGHT expression by reactive T cells rather than LT (Lee et al., 2006), thus presumably in the absence of LTi cells. We observed that RORγt-deficient mice generated an increased number of mature germinal center–containing iBALTs in response to influenza A virus infection as compared with infected wild-type controls (Fig. 2 A). Similarly, in the colon, exposure to DSS induced a threefold higher number of mature tLTs, as well as extensive neutrophil infiltration, in RORγt-deficient mice as compared with control mice (Fig. 2 B and Fig. S1). Interestingly, an increased number of tLTs is present already in unexposed RORγt-deficient mice (Fig. 2 C). These data show, first, that tLTs can be efficiently generated in the absence of LTi cells during infection and inflammation and, second, that the intestinal environment is prone to spontaneous tLT formation in RORγt-deficient mice that lack LNs, PPs, ILFs, and several IL-17– and/or IL-22–producing lymphoid cells (Ivanov et al., 2006; Satoh-Takayama et al., 2008; Sanos et al., 2009).
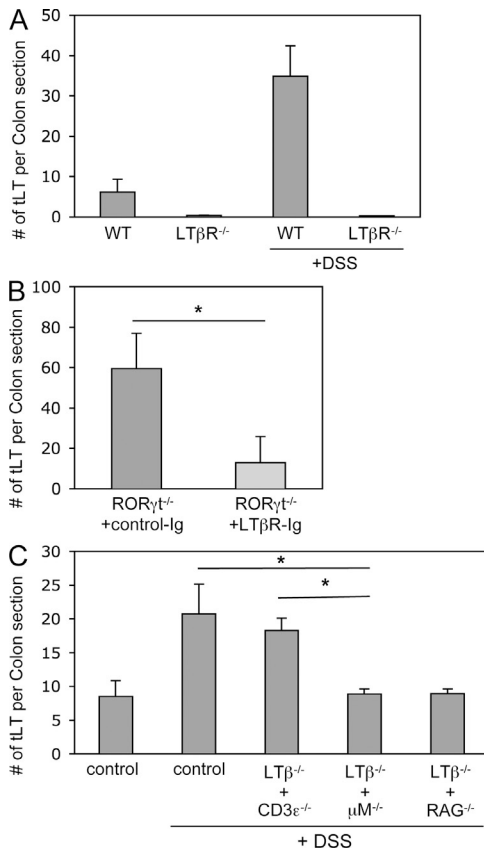
Figure 3.   The LTi function of B cells. (A) Quantification of tLTs in the colons of LTβR-deficient and wild-type control mice that were either untreated or treated with two cycles of 2.5% DSS. Data are shown for one representative experiment out of two with three mice per group. (B) Quantification of colonic tLTs in RORγt$^{-/-}$ mice that were treated with two cycles of 2.5% DSS and by weekly i.p. injections of LTβR-Ig fusion protein or control Ig. Data are shown for one representative experiment out of two with six mice per group. *, P < 0.005. (C) Quantification of tLTs in the colon of wild-type mice and mixed bone marrow chimeras after two cycles with 2% DSS. For mixed bone marrow chimeras, irradiated adult C57BL/6 wild-type mice received bone marrow from LTβ$^{-/-}$ mice that was mixed 1:1 with bone marrow from μM$^{-/-}$, CD3ε$^{-/-}$, or RAG$^{-/-}$ mice to create mice that lack LTβ expression in B cells, T cells, or both B and T cells. DSS treatment was initiated 6 wk after transfer. Data are shown for one representative experiment out of three with five mice per group. *, P < 0.001. Statistical significance was assessed by the paired Student's *t* test. Error bars are SD.
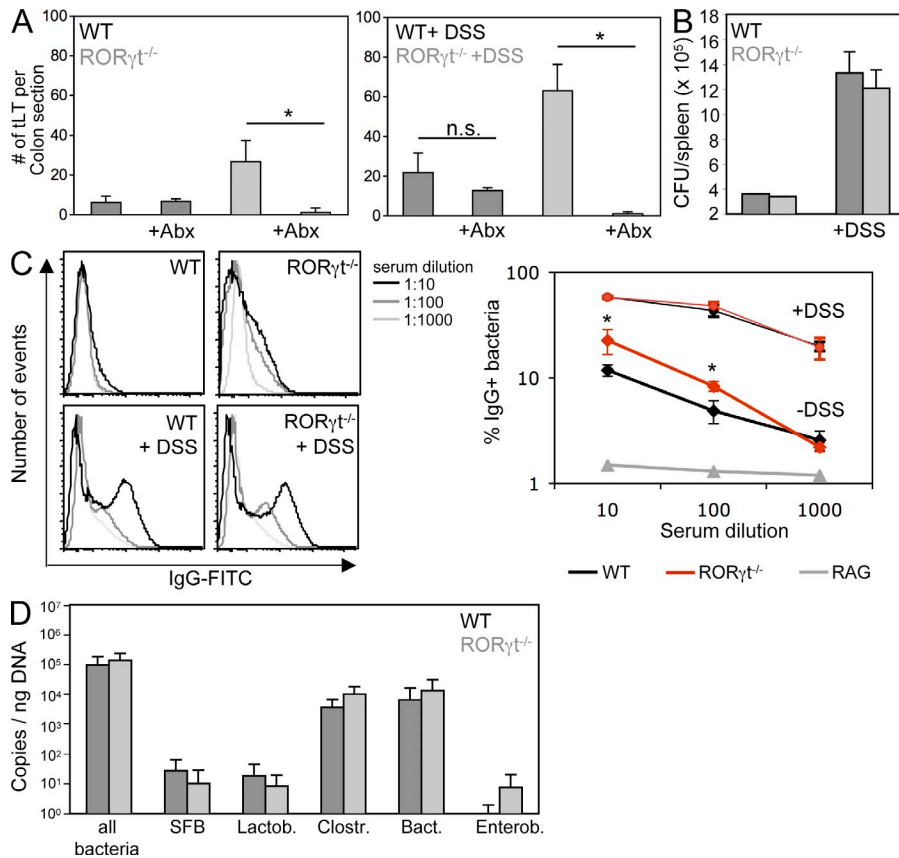
An LTi function for B cells

We first assessed whether tLTs generated during DSS-mediated colitis were induced through the canonical LTβR pathway. In both LTβR–deficient mice and RORγt-deficient mice treated with LTβR-Ig fusion protein, the induction of tLTs during DSS-mediated colitis was markedly inhibited (Fig. 3, A and B). LTβR has two known ligands, LTα$_1$β$_2$ and LIGHT (Gommerman and Browning, 2003). Whereas LTα$_1$β$_2$ is required for the LTi–mediated generation of LNs, PPs, and ILFs (Hamada et al., 2002; Mebius, 2003; Eberl and Littman, 2004), LIGHT is involved in the T cell–mediated generation of

tLTs in the pancreas of aged NOD mice (Lee et al., 2006). As tLTs generated in the colon of DSS-treated mice consist mostly of mature B cell follicles, we hypothesized that a subset of B cells expressing LTα$_1$β$_2$ (Ansel et al., 2000) may function as LTi cells in that context. In that regard, it has been reported that LTα$_1$β$_2$-expressing B cells, in addition to LTi cells, are required for the full development of ILFs (Lorenz et al., 2003). Bone marrow chimeras were thus generated that lacked expression of LTβ on T cells, on B cells, or both. In the absence of LTβ expressed by T cells, the number of tLTs induced during colitis was similar to the number of tLTs induced in unmanipulated wild-type mice (Fig. 3 C). In contrast, in the absence of LTβ expressed by B cells, or both B and T cells, the number of tLTs dropped to the number of tLTs generated in the absence of colitis. Thus, DSS-mediated colitis induces the formation of tLTs through the LTi function of LTα$_1$β$_2$-expressing B cells. Nevertheless, it remains formally possible that LTα$_1$β$_2$-expressing cells types, in addition to lymphocytes, are involved in the formation of tLTs during DSS-mediated colitis in the absence of LTi cells, although no such cells have been identified yet.

Containment of microbiota in the absence of RORγt$^+$ cells

Despite the absence of LTi cells, RORγt-deficient mice develop significantly higher numbers of mature intestinal tLTs, both during steady state and exposure to DSS (Fig. 2, B and C). As DSS-mediated colitis is dependent on microbiota (Hans et al., 2000) and RORγt-deficient mice lack lymphoid tissues and cells involved in intestinal homeostasis and defense (Eberl and Littman, 2004; Eberl et al., 2004; Ivanov et al., 2006; Satoh-Takayama et al., 2008; Eberl and Lochner, 2009; Sanos et al., 2009), we assessed whether microbiota was responsible for the increased lymphoid tissue genesis. In RORγt-deficient mice treated with a large-spectrum cocktail of antibiotics during exposure to DSS, induction of tLTs was abrogated (Fig. 4 A). The induction of tLTs was also abrogated in antibiotic-treated RORγt-deficient mice during steady state. In contrast, antibiotics had no visible effect on the generation of lymphoid tissues in the colon of wild-type mice during steady state, indicating that several of these colonic lymphoid tissues are LTi cell dependent and programmed lymphoid tissues, such as colonic patches (Eberl and Lochner, 2009) and, thus, not tLTs.

We next assessed whether the microbiota-induced formation of tLTs in RORγt-deficient mice was a consequence of decreased containment of the intestinal microbiota. It was recently reported that mice deficient in both Myd88 and TRIF, which are involved in the signaling of toll-like receptors, show deficient containment of the microbiota (Slack et al., 2009). As a consequence, an increased number of live bacteria was recovered from the spleen, and microbiota-specific IgG was detected in the serum. Although exposure to DSS increased the number of live bacteria found in the spleen, no significant difference was observed between RORγt-deficient mice and wild-type controls during steady state and colitis (Fig. 4 B). In contrast, markedly higher titers of serum IgG directed

128

LTi-independent lymphoid tissues in severe colitis | Lochner et al.

Figure 4. Containment of microbiota in the absence of RORγt+ cells. (A) RORγt−/− and wild-type control mice were treated from birth with a cocktail of antibiotics. 8-wk-old mice were exposed or not to two cycles of DSS before quantification of tLTs. Data are shown for one representative experiment out of two with five mice per group. *, P < 0.0001. Statistical significance was assessed by the paired Student's t test. n.s., not significant; Abx, antibiotic treated. (B) The bacterial content in the spleen of RORγt−/− and wild-type control mice was determined by plating spleen extracts from three individual mice exposed or not to DSS on blood agar plates. CFU, colony forming unit. Data are shown for one representative experiment out of two. (C) The IgG response specific for intestinal bacteria was determined in the sera from the peripheral blood of RORγt−/− and wild-type control mice exposed or not to DSS. Data from one representative experiment out of three and three mice per group show the percentage of bacteria positive for IgG binding. *, P < 0.05. As a baseline control, bacteria were directly stained with anti–mouse IgG without the addition of serum (not depicted). (D) Colon biofilms were collected from 8-wk-old RORγt−/− and wild-type control mice and the bacterial content was determined by quantitative PCR. Data are shown for one representative experiment out of two with five mice per group. SFB, segmented filamentous bacteria; Lactob, Lactobacillaceae; Clostr, Clostridiales; Bact, Bacteroides; Enterob, Enterobacteriaceae. Error bars are SD.

against bacterial microbiota were found in RORγt-deficient mice at steady state, a difference which nevertheless vanished during colitis (Fig. 4 C). Thus, although wild-type mice can contain microbiota during steady state without the formation of large numbers of intestinal tLTs and increased serum IgG, RORγt-deficient mice need to increase the number of intestinal tLTs and the production of systemic microbiota–specific IgG to reach a similar levels of containment. Furthermore, upon epithelial damage, RORγt-deficient mice required even larger numbers of intestinal tLTs to be able to develop a level of containment comparable to that of wild-type mice. In that context, the bacterial microbiota was not significantly different between wild-type and RORγt-deficient mice (Fig. 4 D), indicating that RORγt-deficient mice were still able to develop a level of selective pressure on the microbiota that was comparable to the selective pressure developed by wild-type mice.
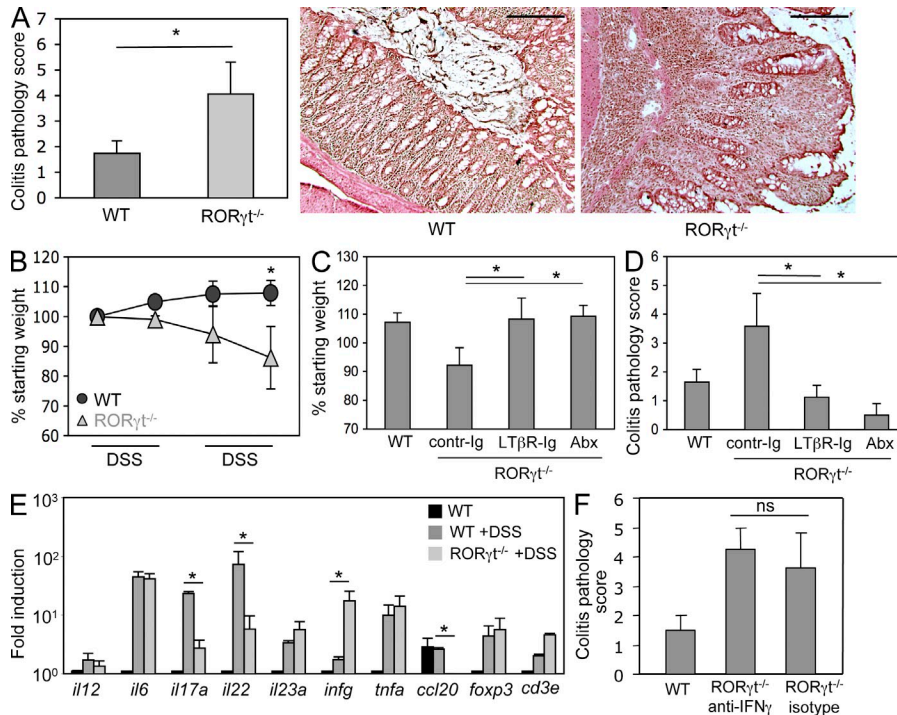
Supernumerary tLTs exacerbate colonic pathology

Even though an increased number of intestinal tLTs may compensate for the immunodeficiencies of RORγt-deficient mice, at least for the containment of the intestinal microbiota, this comes at a high cost for the organism. When exposed to DSS, and in our experimental conditions (Fig. 1 A), RORγt-deficient mice developed severe colitis (Fig. 5 A) and wasting disease (Fig. 5 B), whereas wild-type mice developed a mild colitis and no wasting disease. The severe colitis and wasting disease developing in RORγt-deficient mice was prevented by the administration of antibiotics, as expected, as well as by blocking the formation of tLTs with LTβR-Ig fusion protein (Fig. 5, C and D; and Fig. S2; Rennert et al., 1998). These data demonstrate that the supernumerary intestinal tLTs exacerbate the inflammatory pathology caused by the intestinal microbiota in DSS-treated RORγt-deficient mice.

Furthermore, in the absence of RORγt required for the generation of several IL-17− and/or IL-22–producing lymphoid cells (Ivanov et al., 2006; Satoh-Takayama et al., 2008; Sanos et al., 2009), the intestinal immune response to DSS shifted from a Th17 type of response to a IFN-γ–dominated Th1 type of response (Fig. 5 E, Fig. S3 A, and Fig. S4). However, neutralization of IFN-γ in DSS-treated RORγt-deficient mice did not protect from severe colitis (Fig. 5 F) and had no impact on the number of tLTs (Fig. S3B). In contrast, complementation of RORγt-deficient mice with RORγt-sufficient spleen cells, but not RORγt-deficient cells, partially protected from colitis (Fig. S5), indicating that RORγt+ cells contribute to protection from pathology and thus are involved in intestinal homeostasis. Together, these data show that in the absence of RORγt+ cells, including Th17 cells and lymphoid tissues induced by RORγt+ LTi cells, mice develop aggravated colitis induced by microbiota and supernumerary tLTs.

Figure 5. tLTs aggravate DSS-mediated colitis. (A) Histological disease score in RORγt$^{-/-}$ and wild-type control mice exposed to two cycles of DSS. Scores are shown for eight mice per group from three independent experiments. *, P < 0.01. H&E staining of representative sections from distal colon of RORγt$^{-/-}$ and wild-type control mice after exposure to two cycles of DSS is shown. Bars, 200 μm. (B) Wasting disease. RORγt$^{-/-}$ and wild-type control mice were exposed to DSS cycles as indicated, and mouse body weight was assessed at the beginning of every cycle. Shown are weights relative to the starting weight. Data derive from eight mice per group from three independent experiments. *, P < 0.01. (C and D) LTβR blockade ameliorates DSS colitis. Wild-type and RORγt-deficient mice were exposed to two cycles of DSS. RORγt$^{-/-}$ mice were either treated by weekly i.p. injections of LTβR-Ig protein or with a control Ig. One group of RORγt$^{-/-}$ mice was treated from birth with a cocktail of antibiotics. Data are shown for six mice per group from two to three independent experiments. *, P < 0.01. Shown is mouse weight at the end of the second DSS cycle in percentage of the starting weight (C) and histological disease score (D). Abx, antibiotic treated. (E) Quantitative real-time PCR on whole colon tissue from untreated wild-type controls and RORγt$^{-/-}$, as well as wild-type control mice after exposure to DSS. Ct values were normalized to *Gapdh* expression. Data shown are for one representative experiment out of three with two mice per group. *, P < 0.05. (F) RORγt$^{-/-}$ mice were treated with two i.p. injections of 250 μg of neutralizing anti–IFN-γ antibody before the first and the second DSS cycle. Data are shown for one representative experiment out of two with three mice per group. ns, not specific. P > 0.05. Statistical significance was assessed by the paired Student's *t* test. Error bars are SD.

Hyperactive tLTs and B cells as a cause of aggravated colonic pathology

Intestinal tLTs, as ILFs, are primarily B cell follicles harboring a germinal center but no distinct T cell zone (Fig. 1 B; Eberl and Lochner, 2009). We therefore tested whether tLTs aggravate colonic pathology in DSS–treated RORγt-deficient mice by inducing a hyperactive B cell compartment. In accordance with this view, tLTs in such mice express a 30-fold increase in transcripts for the activation-induced deaminase AID (Fig. 6 A), which is required for gene switch recombination and somatic hypermutation of Ig genes (Muramatsu et al., 2000). Possibly as a consequence, even though it is difficult to assess, IgG$^+$ B cells were present in the lamina propria of DSS-treated RORγt-deficient mice but not in wild-type mice (Fig. 6 B). To demonstrate that Igs were involved in the pathology induced by tLTs, we treated RORγt-deficient mice concomitantly with DSS and IVIG, which have a therapeutic effect against a broad range of hematological and immunological disorders, essentially through the saturation and activation of Fc receptors (Nimmerjahn and Ravetch, 2008). IVIG treatment significantly decreased the colonic pathology induced by tLTs in RORγt-deficient mice (Fig. 6 C). Together, our data indicate that in the absence of RORγt, the supernumerary tLTs induced by the microbiota are nurturing a hyperactive B cell compartment that contributes to the aggravated colonic pathology.

DISCUSSION

tLTs form within numerous types of chronic inflammatory lesions (Aloisi and Pujol-Borrell, 2006) and have been shown to function like secondary lymphoid tissues in the induction of effector B and T cells (Lee et al., 2006; Moyron-Quiroz et al., 2006; Nasr et al., 2007). These inducible tissues can provide protection to virus infection in the absence of LNs or aggravate inflammatory disease. Therefore, in the latter context, it has been suggested that the formation of tLTs may be blocked as a strategy to prevent or mitigate inflammatory disease. The development of LNs and PPs in the fetus (Eberl et al., 2004), and of ILFs in the intestinal lamina propria (Eberl and Littman, 2004), requires RORγt$^+$ LTi cells, and in the absence of RORγt, these lymphoid tissues do not develop. RORγt is also required to generate the proinflammatory Th17 cells (Ivanov et al., 2006) and IL-22–producing NKp46$^+$ innate lymphoid cells (Satoh-Takayama et al., 2008; Luci et al., 2009). Thus, it has been suggested that RORγt antagonists may be developed to block excessive immunity and chronic inflammation in several pathological settings. However, the role of RORγt$^+$ LTi cells in the formation of tLTs during inflammation remained to be clearly assessed, and the effect of an absence of functional RORγt, which is involved in the generation of both lymphoid tissues and Th17 cells, must be carefully measured during inflammatory disease.
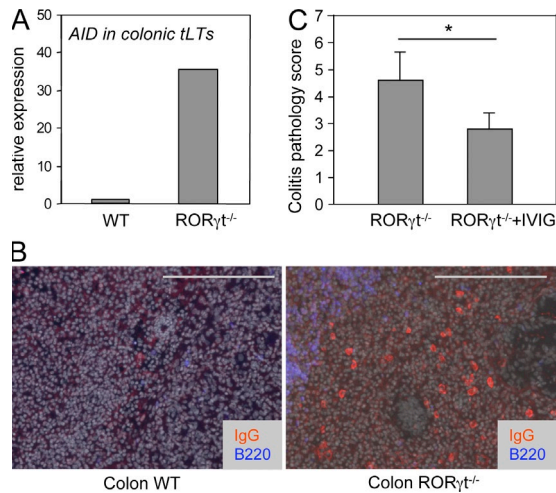
Figure 6. Hyperactive tLTs and B cells as a cause of aggravated colonic pathology. RORγt$^{-/-}$ and wild-type control mice were treated with two cycles of 2.5% DSS. (A) The expression of AID was assessed by quantitative RT-PCR in laser-captured tLTs from DSS-treated RORγt$^{-/-}$ and wild-type control mice. Data are shown for one representative experiment out of two with two mice per group. Ct values were normalized to *Gapdh* expression. (B) Colon sections were stained for IgG, B220, and DAPI for nuclear staining (shown in gray). IgG$^+$ B plasma cells express low levels of B220. Bars, 200 μm. Data are shown for one representative experiment out of two with three mice per group. (C) RORγt$^{-/-}$ mice were treated with two i.p. injections of IVIG. The histological disease score was assessed as described in Materials and methods. Data are shown for one representative experiment out of two with two to three mice per group. Statistical significance was assessed by the paired Student's *t* test. *, P < 0.05. Error bars are SD.

We find that during colitis induced by DSS, mature colonic tLTs develop that consist of a well structured B cell follicle containing predominantly IgM$^+$ B cells and a germinal center. Similar tLTs termed iBALTs were reported in influenza A–infected lungs (Moyron-Quiroz et al., 2004). In the absence of LTi cells in RORγt-deficient mice, both iBALT and colonic tLTs develop, indicating that other cells can take over the function of LTi cells for the induction of lymphoid tissues. In the case of tLTs induced in the pancreas of aged NOD mice, the LTi function is taken over by autoreactive T cells (Lee et al., 2006). Central to the development of LNs, PPs, and ILFs is LTβR-mediated activation of stromal cells by LTα$_1$β$_2$-expressing LTi cells (Mebius, 2003). Activated stromal cells produce the structural chemokines CC19, CCL21, and CXCL13, which are involved in the recruitment and organization of lymphocytes and DCs (Dejardin et al., 2002). In the inflamed pancreas, T cells induce the formation of tLTs through the alternative LTβR ligand LIGHT (Lee et al., 2006). The formation of iBALTs is independent of LTα (Moyron-Quiroz et al., 2004), and the involvement of LIGHT remains to be assessed. In the case of DSS-induced colonic tLTs, B cells perform the LTi function through LTβ, and thus, presumably, through its membrane-bound LTα$_1$β$_2$ heterotrimer. Together, these data show that tLTs can develop during chronic inflammation through similar mechanisms but distinct lymphocyte or lymphoid cell subsets.

We show that the formation of tLTs in RORγt–deficient mice is induced by microbiota through the LTi function of B cells, even though we do not formally exclude an LTi function for other cell types in that context. So how does microbiota induce the recruitment of LTβ$^+$ B cells? We had shown previously that CCL20 was required for the recruitment of B cells and the formation of ILFs (Bouskra et al., 2008) but expression of CCL20 was undetectable in RORγt–deficient mice. The only cytokine found to be increased in RORγt–deficient mice treated with DSS was IFN-γ; however, blocking IFN-γ with neutralizing antibody had no effect on the number of tLTs and the severity of disease. The intestine of DSS-treated RORγt-deficient mice nevertheless showed an important infiltration of IgG$^+$ B cells. We therefore suggest that the microbiota-induced inflammation unfolding in DSS-treated RORγt-deficient mice eventually leads to the sustained recruitment of B cells, which induce the formation of tLTs through their expression of LTα$_1$β$_2$. Given that tLTs are primarily B cell follicles, this pathway can generate a positive-feedback loop in B cell activation and differentiation and in the formation of tLTs.

In RORγt-deficient mice during steady state or that have been exposed to DSS, a vast network of tLTs develops that contains approximately three times the number of tLTs found in wild-type mice subjected to the same treatments. RORγt is required for the development of LNs and PPs, as well as for the generation of a collection of lymphoid cells producing IL-17 and/or IL-22, such as Th17 cells and IL-22$^+$ NKp46$^+$ cells. The latter cell type was recently shown to be involved in protection against infection by *Citrobacter rodentium* and DSS-induced colitis (Satoh-Takayama et al., 2008), and IL-17 and IL-22 synergize in the activation of epithelial cells to produce antibacterial peptides (Liang et al., 2006). Thus, it might be expected that the absence of lymphoid tissues and of IL-17/22–producing lymphoid cells in RORγt-deficient will be matched by the increased activity in other immune compartments, such as tLT formation, to maintain a similar level of containment of the intestinal microbiota. Such a compensatory mechanism has been reported by Lorenz et al. (2003); the inhibition of development of secondary lymphoid tissues through the administration of LTβR-Ig protein to pregnant mothers induced the formation of numerous tLTs or ILFs. However, when exposed to DSS, which injures the epithelial cell layer, RORγt-deficient mice appear only to be able to contain microbiota at the price of an additional increase in intestinal tLTs and B cell activity. This increase in the number of tLTs and in B cell activity is, however, not tolerated by the intestine, which develops severe inflammation and leads the host to wasting disease. This pathology is possibly a consequence of the formation of immune complexes consisting of bacteria and specific IgG, which activate IgG receptor-bearing inflammatory cells, such as neutrophils. This hypothesis is supported by the antiinflammatory effect of IVIG treatment, which is shown to depend on IgG receptors (Nimmerjahn and Ravetch, 2008).

RORγt controls the proinflammatory IL-17 pathway (Ivanov et al., 2006), which is shown to be involved in auto-immune pathology through the recruitment of neutrophils (Weaver et al., 2006). The IL-17/23 pathway is involved in several colitis models in mice (Uhlig and Powrie, 2009), and patients with a defective IL-23R show resistance to the development of the disease (Duerr et al., 2006). Therefore, it can be expected that the absence of RORγt, or antagonizing RORγt function during the initial phase of inflammation, protects from progression to inflammatory disease. We show that colitis induced by exposure to DSS was actually more severe in RORγt-deficient mice as compared with RORγt-sufficient mice. In the absence of RORγt, the colon developed profound tissue damage, and mice suffered from marked wasting disease, whereas in the presence of RORγt, mice endured mild intestinal inflammation under the regimen applied and grew normally. Furthermore, complementation of RORγt-deficient mice with RORγt-sufficient spleen cells significantly decreased the severity of the disease, demonstrating a protective effect of RORγt$^+$ cells in intestinal pathology. We suggest that RORγt$^+$ cells, including Th17 cells and IL-22–producing NKp46$^+$ cells, limit DSS-induced intestinal inflammatory disease by strengthening antibacterial immunity, such as the production of antibacterial peptides by epithelial cells (Liang et al., 2006). Thus, our data show that a narrow road has to be followed to prevent the pathological effect of immunity during colitis while maintaining the essential functions of immunity for intestinal homeostasis and defense.

MATERIALS AND METHODS

Mice. RORγt-deficient (*Rorc*(γt)$^{Gfp/Gfp}$) mice (Eberl et al., 2004) and BAC transgenic *Rorc*(gt)-*Gfp*^{TG} mice (Lochner et al., 2008) have been described previously. Mice deficient in LTβR (Fütterer et al., 1998), LTβ (Alimzhanov et al., 1997), mu chain (Kitamura et al., 1991), CD3 epsilon (Malissen et al., 1995), and RAG2 (Shinkai et al., 1992) have been described before. All mice were kept in specific pathogen-free conditions and all animal experiments were approved by the committee on animal experimentation of the Institut Pasteur and by the French Ministry of Agriculture.

In vivo treatments. For antibiotic treatment, pregnant mothers were treated with a mixture of 1 mg/ml ampicillin, 1 mg/ml colistin, and 5 mg/ml streptomycin together with 5% glucose (all from Sigma-Aldrich) in their drinking water. After birth, treatment was continued until analysis. For LTβR-Ig treatment, mice were treated with LTβR-Ig fusion protein (gift from J. Browning, Biogen Idec, Cambridge, MA; Browning et al., 1997) by weekly i.p. injections of 10 μg/mg of body weight during the course of the experiment. Control mice were treated with the Ig fusion partner. For IFN-γ neutralization, mice received two i.p. injections of 250 μg of neutralizing anti–IFN-γ (clone R4-6A2; eBioscience) or isotype control antibodies before the first and second DSS cycle. Colitis was induced using DSS salt (mol wt = 36,000–50,000; MP Biomedicals) dissolved in the drinking water at a concentration of 2.5% (m/v). Mice were exposed to DSS for 7 d, followed by a recovery period of 10 d without DSS. This cycle was repeated once or twice and weight was monitored at the end of every cycle. For IVIG treatment, DSS-treated mice received two i.v. injections of Gamunex 10% (Talecris Biotherapeutics) at a concentration of 1 g/kg at the end of a first DSS cycle (day 5) and 1 d before a second DSS cycle (day 11).

Quantification of tLTs. Whole colons were frozen as swiss rolls in OCT compound 4583 (Sakura) and frozen blocks were cut as 7-μm sections.

40 sections of a whole colon were taken at regular intervals and fixed for 5 min in acetone at −20°C. For staining, slides were first hydrated in PBS-BS (PBS containing 1% normal bovine serum; Sigma-Aldrich) for 5 min and blocked with 10% bovine serum in PBS for 1 h at room temperature. Slides were then incubated with anti-phycoerythrin–conjugated anti-CD45R/B220 mAb (clone RA3-6B2) in PBS-BS at room temperature for 1 h, washed three times for 5 min with PBS-BS, incubated with DAPI (Sigma-Aldrich) for 5 min at room temperature, washed three times for 5 min, and mounted with Fluoromount-G (SouthernBiotech). Numbers of tLTs per colon section were calculated as the mean number of tLTs per section in 40 sections.

Influenza virus A infection. Mice were infected intranasally with 50 PFU influenza A virus (H3N2 strain Scotland/20/74). Mice were sacrificed 21 d after infection.

Immunofluorescence histology. For immunofluorescence histology, tissues were fixed and stained as previously described (Peduto et al., 2009). In brief, tissues were washed and fixed overnight at 4°C in a fresh solution of 4% paraformaldehyde (Sigma-Aldrich) in PBS. The samples were then washed for 1 d in PBS, incubated in a solution of 30% sucrose (Sigma-Aldrich) in PBS, and embedded in OCT. Frozen blocks were cut at 8-μm thickness and sections collected onto Superfrost Plus slides (VWR). For staining, slides were first hydrated in PBS-XG (PBS containing 0.1% Triton X-100 and 1% normal goat serum; Sigma-Aldrich) for 5 min and blocked with 10% bovine serum in PBS-XG for 1 h at room temperature. Slides were then incubated with primary polyclonal antibody or conjugated mAb (in general 1/100) in PBS-XG overnight at 4°C, washed three times for 5 min with PBS-XG, incubated with DAPI for 5 min at room temperature, washed three times for 5 min, and mounted with Fluoromount-G. Slides were examined under a fluorescence microscope (AxioImager M1; Carl Zeiss, Inc.) equipped with a charge-coupled device camera and images were processed with AxioVision software (Carl Zeiss, Inc.).

Laser capture microdissection. Colon tissues were embedded in OCT compound 4583 (Sakura), frozen in a bath of isopentane cooled with liquid nitrogen, and stocked at −80°C. Frozen blocks were cut at 10-μm thickness and serial sections collected onto Superfrost/Plus slides. Sections were immediately fixed for 5 min in acetone at −20°C, dried, and stored at −80°C. Serial sections were then thawed and immediately stained for 5 s with histogen (MDS Analytical Technologies), washed briefly in RNase-free water supplemented with ProtectRNA (Sigma-Aldrich), dehydrated successively in one bath of 70% ethanol for 30 s, two baths of 95% ethanol for 1 min, two baths of water-free ethanol (VWR) for 2 min, and two baths of xylene for 5 min, and air-dried. Slides were transferred immediately into a Veritas Laser Capture Microdissector (MDS Analytical Technologies), microdissected, and captured with Capsure Macro LCM caps (MDS Analytical Technologies). RNA was isolated using the PicoPure RNA Isolation kit (MDS Analytical Technologies), and its quality was assessed using the 2100 Bioanalyzer system (Agilent Technologies).

Antibodies. The following mAbs were purchased from BD: PE-conjugated anti–mouse IgM (R6-60.2); from eBioscience: allophycocyanin-conjugated anti-CD45R/B220 (RA3-6B2), PE-conjugated anti-CD106 (VCAM-1; 429), anti-CD11c (N418), anti-IgA (11–44-2), biotinylated anti–Ly-77 (GL7), and purified anti-CD3ε (500A2); and from Serotec: biotinylated anti-neutrophil (7/4). Cy3-anti–armenian or –syrian hamster and DyLight 488 donkey anti–mouse IgG were purchased from Jackson Immuno-Research Laboratories. Cy3-conjugated streptavidin was purchased from Sigma-Aldrich.

Colitis disease score. Swiss rolls of whole colons were directly frozen in OCT and sections of 7-μm thickness were stained with hematoxylin and eosin (H&E). Histological scoring was performed using a modified scoring system described previously (Hartmann et al., 2000). In brief, the presence of rare inflammatory cells in the lamina propria were counted as: 0, increased numbers of inflammatory cells; 1, confluence of inflammatory cells; 2, extending

into the submucosa; and 3, transmural extension of the inflammatory cell infiltrate. For epithelial damage, absence of mucosal damage was counted as 0, discrete focal lymphoepithelial lesions were counted as 1, mucosal erosion/ulceration was counted as 2, and a score of 3 was given for extensive mucosal damage and extension through deeper structures of the bowel wall. The two subscores were added and the combined histological score ranged from 0 (no changes) to 6 (extensive cell infiltration and tissue damage).

RNA isolation and quantitative PCR. To perform gene expression analysis, whole tissue from the middle and terminal part of the colon was immediately frozen in liquid nitrogen upon animal sacrifice. Tissue was homogenized using Ultra Turrax T8 (IKA-Werke) in TRIZOL regent, and total RNA was purified according to the manufacturer's protocol (Invitrogen). RNA was subjected to DNase I digestion and additional purification using the RNeasy Mini kit (QIAGEN). 1 µg of total RNA was transcribed into cDNA using Superscript III reverse transcription (Invitrogen) according to the manufacturer's protocol. Quantitative real-time PCR was performed using RT^2 qPCR Primer sets and RT^2 SYBR-Green master mix (QIAGEN) on a PTC-200 thermocycler equipped with a Chromo4 detector (Bio-Rad Laboratories). Data were analyzed using Opticon Monitor software (Bio-Rad Laboratories).

Bone marrow and spleen transfer. 10^7 bone marrow cells from $CD3\varepsilon^{-/-}$, $\mu M^{-/-}$, or $RAG^{-/-}$ mice were mixed with 10^7 bone marrow cells from $LT\beta^{-/-}$ mice and injected i.v. into 10-Gy irradiated wild-type mice. After 4 wk, reconstitution of the mice was assessed in peripheral blood. In reconstituted mice, DSS-mediated colitis experiments were performed 6 wk after transfer. For spleen transfer, $ROR\gamma t^{-/-}$ mice were sublethally irradiated (500 rad) and transferred with 10^7 splenocytes from either RORγt-deficient or RORγt-sufficient littermate mice. 10 d later, mice were treated with two cycles of DSS.

Intestinal biofilm collection and analysis. Large intestine was isolated immediately after animal sacrifice. Fecal contents were removed using forceps pressed along the whole length of the organ, and the tissue was placed into a Petri dish containing sterile ice-cold PBS. The intestine was cut into ∼3-cm sections and then cut longitudinally and vigorously rinsed with scraping using a Pasteur pipette. Tissue was then removed and PBS containing the mucosal biofilm was transferred to a 50-ml falcon tube. Biofilm was separated by centrifugation for 15 min at 4,000 rpm and 4°C, and the supernatant was discarded. DNA extraction was performed using FastDNA Spin kit (MP Biomedicals) using Lysis buffer CLS-Y, according to the manufacturer's instructions. Quantitative PCR was performed on a DNA Engine thermal cycler (Bio-Rad Laboratories). QuantiTect SYBR green (QIAGEN) master mix was used in 25-µl reactions. Primers and reaction conditions were described previously (Bouskra et al., 2008). Absolute numbers of bacteria were determined from standard curves established by quantitative PCR with serial dilutions of reference plasmids harboring 16S rDNA.

Bacterial IgG FACS. Mouse serum was diluted 10-fold in PBS and heat-inactivated at 60°C for 30 min. After centrifugation (10 min, 13,000 rpm in a Microcentrifuge; Eppendorf), the supernatant was further diluted through 1:10 serial dilutions in PBS. To isolate fecal bacteria, ∼0.1 g of feces from RAG-2–deficient mice was suspended in 1 ml PBS and spun on lowest setting to remove fecal matter. 20 µl of supernatant was collected and washed with PBS (1 min at 8,000 rpm). Bacteria were stained with DAPI 1 µg/ml for 5 min and washed twice with PBS. Bacteria were then resuspended in 25 µl PBS and 25 µl of serum dilutions was added. After 1 h of incubation on ice, bacteria were washed twice and stained with DyLight488 anti–mouse-IgG Antibody (Jackson) for 30 min at 4°C. After washing twice, bacteria were resuspended in PBS 1% PFA and analyzed on a FACSCanto II cytometer (BD).

Counting bacterial CFU in the spleen. Spleens were pressed through a 70-µm cell strainer into 2 ml PBS and cells were resuspended by pipetting several times up and down. 100 µl of cell suspension was mixed with 900 µl PBS/0.1% Triton X-100, and 10 µl of this dilution was plated as triplicates

on Brucella agar plates containing 5% horse blood. Colonies were counted after 2 d of culture at 37°C.

Online supplemental material. Fig. S1 shows the structure of tLTs and neutrophil recruitment in DSS-treated RORγt–deficient mice. Fig. S2 shows the histology of the effect of LTβR-Ig and antibiotics on colitis progression. Fig. S3 shows the increased expression of IFN-γ by $CD4^+$ T cells and the lack of impact of neutralizing IFN-γ in disease severity. Fig. S4 shows the expression of transcripts for LIGHT, LTα, LTβ, and LTβR in colonic tissue. Fig. S5 shows the effect of RORγt-sufficient spleen cells upon transfer into irradiated RORγt-deficient mice. Online supplemental material is available at http://www.jem.org/cgi/content/full/jem.20100052/DC1.

REFERENCES

Alimzhanov, M.B., D.V. Kuprash, M.H. Kosco-Vilbois, A. Luz, R.L. Turetskaya, A. Tarakhovsky, K. Rajewsky, S.A. Nedospasov, and K. Pfeffer. 1997. Abnormal development of secondary lymphoid tissues in lymphotoxin β–deficient mice. *Proc. Natl. Acad. Sci. USA.* 94:9302–9307. doi:10.1073/pnas.94.17.9302

Aloisi, F., and R. Pujol-Borrell. 2006. Lymphoid neogenesis in chronic inflammatory diseases. *Nat. Rev. Immunol.* 6:205–217. doi:10.1038/nri1786

Ansel, K.M., V.N. Ngo, P.L. Hyman, S.A. Luther, R. Förster, J.D. Sedgwick, J.L. Browning, M. Lipp, and J.G. Cyster. 2000. A chemokine-driven positive feedback loop organizes lymphoid follicles. *Nature.* 406:309–314. doi:10.1038/35018581

Bouskra, D., C. Brézillon, M. Bérard, C. Werts, R. Varona, I.G. Boneca, and G. Eberl. 2008. Lymphoid tissue genesis induced by commensals through NOD1 regulates intestinal homeostasis. *Nature.* 456:507–510. doi:10.1038/nature07450

Browning, J.L., I.D. Sizing, P. Lawton, P.R. Bourdon, P.D. Rennert, G.R. Majeau, C.M. Ambrose, C. Hession, K. Miatkowski, D.A. Griffiths, et al. 1997. Characterization of lymphotoxin-α β complexes on the surface of mouse lymphocytes. *J. Immunol.* 159:3288–3298.

Dejardin, E., N.M. Droin, M. Delhase, E. Haas, Y. Cao, C. Makris, Z.W. Li, M. Karin, C.F. Ware, and D.R. Green. 2002. The lymphotoxin-β receptor induces different patterns of gene expression via two NF-kappaB pathways. *Immunity.* 17:525–535. doi:10.1016/S1074-7613(02)00423-5

Duerr, R.H., K.D. Taylor, S.R. Brant, J.D. Rioux, M.S. Silverberg, M.J. Daly, A.H. Steinhart, C. Abraham, M. Regueiro, A. Griffiths, et al. 2006. A genome-wide association study identifies IL23R as an inflammatory bowel disease gene. *Science.* 314:1461–1463. doi:10.1126/science.1135245

Eberl, G., and D.R. Littman. 2004. Thymic origin of intestinal αβ T cells revealed by fate mapping of $ROR\gamma^+$ cells. *Science.* 305:248–251. doi:10.1126/science.1096472

Eberl, G., and M. Lochner. 2009. The development of intestinal lymphoid tissues at the interface of self and microbiota. *Mucosal Immunol.* 2:478–485. doi:10.1038/mi.2009.114

Eberl, G., S. Marmon, M.J. Sunshine, P.D. Rennert, Y. Choi, and D.R. Littman. 2004. An essential function for the nuclear receptor RORgamma(t) in the generation of fetal lymphoid tissue inducer cells. *Nat. Immunol.* 5:64–73. doi:10.1038/ni1022

Fütterer, A., K. Mink, A. Luz, M.H. Kosco-Vilbois, and K. Pfeffer. 1998. The lymphotoxin β receptor controls organogenesis and affinity maturation in peripheral lymphoid tissues. *Immunity.* 9:59–70. doi:10.1016/S1074-7613(00)80588-9

Gommerman, J.L., and J.L. Browning. 2003. Lymphotoxin/light, lymphoid microenvironments and autoimmune disease. *Nat. Rev. Immunol.* 3:642–655. doi:10.1038/nri1151

Hamada, H., T. Hiroi, Y. Nishiyama, H. Takahashi, Y. Masunaga, S. Hachimura, S. Kaminogawa, H. Takahashi-Iwanaga, T. Iwanaga, H. Kiyono, et al. 2002. Identification of multiple isolated lymphoid follicles on the antimesenteric wall of the mouse small intestine. *J. Immunol.* 168:57–64.

Hans, W., J. Schölmerich, V. Gross, and W. Falk. 2000. The role of the resident intestinal flora in acute and chronic dextran sulfate sodium-induced colitis in mice. *Eur. J. Gastroenterol. Hepatol.* 12:267–273. doi:10.1097/00042737-200012030-00002

Hartmann, G., C. Bidlingmaier, B. Siegmund, S. Albrich, J. Schulze, K. Tschoep, A. Eigler, H.A. Lehr, and S. Endres. 2000. Specific type IV phosphodiesterase inhibitor rolipram mitigates experimental colitis in mice. *J. Pharmacol. Exp. Ther.* 292:22–30.

Honda, K., H. Nakano, H. Yoshida, S. Nishikawa, P. Rennert, K. Ikuta, M. Tamechika, K. Yamaguchi, T. Fukumoto, T. Chiba, and S.I. Nishikawa. 2001. Molecular basis for hematopoietic/mesenchymal interaction during initiation of Peyer's patch organogenesis. *J. Exp. Med.* 193:621–630. doi:10.1084/jem.193.5.621

Ivanov, I.I., B.S. McKenzie, L. Zhou, C.E. Tadokoro, A. Lepelley, J.J. Lafaille, D.J. Cua, and D.R. Littman. 2006. The orphan nuclear receptor RORγt directs the differentiation program of proinflammatory IL-17+ T helper cells. *Cell.* 126:1121–1133. doi:10.1016/j.cell.2006.07.035

Kastelein, R.A., C.A. Hunter, and D.J. Cua. 2007. Discovery and biology of IL-23 and IL-27: related but functionally distinct regulators of inflammation. *Annu. Rev. Immunol.* 25:221–242. doi:10.1146/annurev .immunol.22.012703.104758

Kitamura, D., J. Roes, R. Kühn, and K. Rajewsky. 1991. A B cell–deficient mouse by targeted disruption of the membrane exon of the immunoglobulin mu chain gene. *Nature.* 350:423–426. doi:10.1038/350423a0

Lee, Y., R.K. Chin, P. Christiansen, Y. Sun, A.V. Tumanov, J. Wang, A.V. Chervonsky, and Y.X. Fu. 2006. Recruitment and activation of naive T cells in the islets by lymphotoxin beta receptor–dependent tertiary lymphoid structure. *Immunity.* 25:499–509. doi:10.1016/j.immuni.2006.06.016

Leppkes, M., C. Becker, I.I. Ivanov, S. Hirth, S. Wirtz, C. Neufert, S. Pouly, A.J. Murphy, D.M. Valenzuela, G.D. Yancopoulos, et al. 2009. RORgamma-expressing Th17 cells induce murine chronic intestinal inflammation via redundant effects of IL-17A and IL-17F. *Gastroenterology.* 136:257–267. doi:10.1053/j.gastro.2008.10.018

Liang, S.C., X.Y. Tan, D.P. Luxenberg, R. Karim, K. Dunussi-Joannopoulos, M. Collins, and L.A. Fouser. 2006. Interleukin (IL)-22 and IL-17 are coexpressed by Th17 cells and cooperatively enhance expression of antimicrobial peptides. *J. Exp. Med.* 203:2271–2279. doi:10.1084/jem.20061308

Lochner, M., L. Peduto, M. Cherrier, S. Sawa, F. Langa, R. Varona, D. Riethmacher, M. Si-Tahar, J.P. Di Santo, and G. Eberl. 2008. In vivo equilibrium of proinflammatory IL-17+ and regulatory IL-10+ Foxp3+ RORγt+ T cells. *J. Exp. Med.* 205:1381–1393. doi:10.1084/jem.20080034

Lorenz, R.G., D.D. Chaplin, K.G. McDonald, J.S. McDonough, and R.D. Newberry. 2003. Isolated lymphoid follicle formation is inducible and dependent upon lymphotoxin-sufficient B lymphocytes, lymphotoxin β receptor, and TNF receptor I function. *J. Immunol.* 170:5475–5482.

Luci, C., A. Reynders, I.I. Ivanov, C. Cognet, L. Chiche, L. Chasson, J. Hardwigsen, E. Anguiano, J. Banchereau, D. Chaussabel, et al. 2009. Influence of the transcription factor RORgammat on the development of NKp46+ cell populations in gut and skin. *Nat. Immunol.* 10:75–82. doi:10.1038/ni.1681

Malissen, M., A. Gillet, L. Ardouin, G. Bouvier, J. Trucy, P. Ferrier, E. Vivier, and B. Malissen. 1995. Altered T cell development in mice with a targeted mutation of the CD3-epsilon gene. *EMBO J.* 14:4641–4653.

McGeachy, M.J., Y. Chen, C.M. Tato, A. Laurence, B. Joyce-Shaikh, W.M. Blumenschein, T.K. McClanahan, J.J. O'Shea, and D.J. Cua. 2009. The interleukin 23 receptor is essential for the terminal differentiation of interleukin 17-producing effector T helper cells in vivo. *Nat. Immunol.* 10:314–324. doi:10.1038/ni.1698

Mebius, R.E. 2003. Organogenesis of lymphoid tissues. *Nat. Rev. Immunol.* 3:292–303. doi:10.1038/nri1054

Moyron-Quiroz, J.E., J. Rangel-Moreno, K. Kusser, L. Hartson, F. Sprague, S. Goodrich, D.L. Woodland, F.E. Lund, and T.D. Randall. 2004. Role of inducible bronchus associated lymphoid tissue (iBALT) in respiratory immunity. *Nat. Med.* 10:927–934. doi:10.1038/nm1091

Moyron-Quiroz, J.E., J. Rangel-Moreno, L. Hartson, K. Kusser, M.P. Tighe, K.D. Klonowski, L. Lefrançois, L.S. Cauley, A.G. Harmsen, F.E. Lund, and T.D. Randall. 2006. Persistence and responsiveness of immunologic memory in the absence of secondary lymphoid organs. *Immunity.* 25:643–654. doi:10.1016/j.immuni.2006.08.022

Muramatsu, M., K. Kinoshita, S. Fagarasan, S. Yamada, Y. Shinkai, and T. Honjo. 2000. Class switch recombination and hypermutation require activation-induced cytidine deaminase (AID), a potential RNA editing enzyme. *Cell.* 102:553–563. doi:10.1016/S0092-8674(00)00078-7

Nasr, I.W., M. Reel, M.H. Oberbarnscheidt, R.H. Mounzer, F.K. Baddoura, N.H. Ruddle, and F.G. Lakkis. 2007. Tertiary lymphoid tissues generate effector and memory T cells that lead to allograft rejection. *Am. J. Transplant.* 7:1071–1079. doi:10.1111/j.1600-6143.2007.01756.x

Nimmerjahn, F., and J.V. Ravetch. 2008. Anti-inflammatory actions of intravenous immunoglobulin. *Annu. Rev. Immunol.* 26:513–533. doi:10.1146/annurev.immunol.26.021607.090232

Pabst, O., H. Herbrand, M. Friedrichsen, S. Velaga, M. Dorsch, G. Berhardt, T. Worbs, A.J. Macpherson, and R. Förster. 2006. Adaptation of solitary intestinal lymphoid tissue in response to microbiota and chemokine receptor CCR7 signaling. *J. Immunol.* 177:6824–6832.

Peduto, L., S. Dulauroy, M. Lochner, G.F. Späth, M.A. Morales, A. Cumano, and G. Eberl. 2009. Inflammation recapitulates the ontogeny of lymphoid stromal cells. *J. Immunol.* 182:5789–5799. doi:10.4049/jimmunol.0803974

Rennert, P.D., D. James, F. Mackay, J.L. Browning, and P.S. Hochman. 1998. Lymph node genesis is induced by signaling through the lymphotoxin β receptor. *Immunity.* 9:71–79. doi:10.1016/S1074-7613(00)80589-0

Sanos, S.L., V.L. Bui, A. Mortha, K. Oberle, C. Heners, C. Johner, and A. Diefenbach. 2009. RORgammat and commensal microflora are required for the differentiation of mucosal interleukin 22-producing NKp46+ cells. *Nat. Immunol.* 10:83–91. doi:10.1038/ni.1684

Satoh-Takayama, N., C.A. Vosshenrich, S. Lesjean-Pottier, S. Sawa, M. Lochner, F. Rattis, J.J. Mention, K. Thiam, N. Cerf-Bensussan, O. Mandelboim, et al. 2008. Microbial flora drives interleukin 22 production in intestinal NKp46+ cells that provide innate mucosal immune defense. *Immunity.* 29:958–970. doi:10.1016/j.immuni.2008.11.001

Shinkai, Y., G. Rathbun, K.P. Lam, E.M. Oltz, V. Stewart, M. Mendelsohn, J. Charron, M. Datta, F. Young, A.M. Stall, et al. 1992. RAG-2-deficient mice lack mature lymphocytes owing to inability to initiate V(D)J rearrangement. *Cell.* 68:855–867. doi:10.1016/0092-8674(92)90029-C

Slack, E., S. Hapfelmeier, B. Stecher, Y. Velykoredko, M. Stoel, M.A. Lawson, M.B. Geuking, B. Beutler, T.F. Tedder, W.D. Hardt, et al. 2009. Innate and adaptive immunity cooperate flexibly to maintain host-microbiota mutualism. *Science.* 325:617–620. doi:10.1126/science.1172747

Spahn, T.W., H. Herbst, P.D. Rennert, N. Lügering, C. Maaser, M. Kraft, A. Fontana, H.L. Weiner, W. Domschke, and T. Kucharzik. 2002. Induction of colitis in mice deficient of Peyer's patches and mesenteric lymph nodes is associated with increased disease severity and formation of colonic lymphoid patches. *Am. J. Pathol.* 161:2273–2282.

Uhlig, H.H., and F. Powrie. 2009. Mouse models of intestinal inflammation as tools to understand the pathogenesis of inflammatory bowel disease. *Eur. J. Immunol.* 39:2021–2026. doi:10.1002/eji.200939602

Weaver, C.T., L.E. Harrington, P.R. Mangan, M. Gavrieli, and K.M. Murphy. 2006. Th17: an effector CD4 T cell lineage with regulatory T cell ties. *Immunity.* 24:677–688. doi:10.1016/j.immuni.2006.06.002

Zhang, Z., M. Zheng, J. Bindas, P. Schwarzenberger, and J.K. Kolls. 2006. Critical role of IL-17 receptor signaling in acute TNBS-induced colitis. *Inflamm. Bowel Dis.* 12:382–388. doi:10.1097/01.MIB .0000218764.06959.91